Copy 5

RM A52J17

NACA RM A52J17

DEC 31 1952 UNCLASSIFIED

RESEARCH MEMORANDUM

CORRELATION OF BUFFET BOUNDARIES PREDICTED FROM WIND-TUNNEL TESTS WITH THOSE MEASURED DURING FLIGHT TESTS ON THE F8F-1 AND X-1 AIRPLANES - TRANSONIC-BUMP METHOD

By Andrew Martin and James F. Reed

Ames Aeronautical Laboratory
Moffett Field, Calif.

NATIONAL ADVISORY COMMITTEE FOR AERONAUTICS

WASHINGTON

December 24, 1952

NATIONAL ADVISORY COMMITTEE FOR AERONAUTICS

RESEARCH MEMORANDUM

CORRELATION OF BUFFET BOUNDARIES PREDICTED FROM WIND-TUNNEL TESTS WITH THOSE MEASURED DURING FLIGHT TESTS ON THE F8F-1 AND X-1 AIRPLANES - TRANSONIC-BUMP METHOD

By Andrew Martin and James F. Reed

SUMMARY

Semispan wing-fuselage models of the F8F-1 and X-1 airplanes have been tested in the Ames 16-foot high-speed wind tunnel utilizing the transonic-bump method. Presented for these models are the variations of lift coefficient with angle of attack and Mach number, and pitching-moment coefficient with lift coefficient at various Mach numbers. Fluctuating wing-bending moments and fluctuating total pressures in the wake of the wings were also obtained primarily to aid in the study of the buffeting problem. Buffet boundaries estimated from these fluctuation measurements are in reasonable agreement with flight-determined buffet boundaries, giving evidence that it may be possible to predict the buffet boundaries of full-scale airplanes from wind-tunnel tests of relatively simple models.

INTRODUCTION

One of the first factors of concern in the study of buffet characteristics of airplanes is the establishment of conditions of lift coefficient and Mach number at which airplane buffeting occurs. Flight tests to determine buffet boundaries have been conducted with various airplanes. Buffet boundaries have been correlated with airfoil-section characteristics in reference 1. These airfoil-section characteristics were either obtained from wind-tunnel airfoil-section data or calculated using theoretical airfoil-section data.

As a supplement to static force tests of relatively simple models of the F8F-1 and X-1 airplanes on the transonic bump of the Ames 16-foot wind tunnel, fluctuating wing-bending moments and fluctuating total pressures in the wake of the wings were measured. These fluctuation measurements were correlated with flight-determined buffet boundaries.

[redacted]

NOTATION

C_B bending-moment coefficient $\left[\frac{\text{bending moment}}{q(S/2)(b/2)}\right]$

ΔC_B double amplitude of bending-moment coefficient fluctuations

C_L lift coefficient $\left[\frac{\text{semispan lift}}{q(S/2)}\right]$

C_m pitching-moment coefficient, referred to 0.25 $\bar{c}$ $\left[\frac{\text{semispan pitching moment}}{q(S/2)\bar{c}}\right]$

$\frac{\Delta h}{q}$ pressure-fluctuation coefficient

A aspect ratio $\left(\frac{b^2}{S}\right)$

M Mach number at 0.25 mean aerodynamic chord position

M_L local Mach number

R Reynolds number based on mean aerodynamic chord

S total wing area (twice wing area of semispan model), square feet

V free-stream velocity, feet per second

b twice span of semispan model, feet

c local wing chord, feet

$\bar{c}$ mean aerodynamic chord $\left(\frac{\int_0^{b/2} c^2 dy}{\int_0^{b/2} c\, dy}\right)$, feet

h average total-pressure loss in wake, pounds per square foot

Δh double amplitude of total-pressure fluctuations in the wake, pounds per square foot

q dynamic pressure $\left(\frac{1}{2}\rho V^2\right)$, pounds per square foot

y spanwise distance from plane of symmetry, feet

[redacted]

α angle of attack of root chord, degrees

ρ air density, slugs per cubic foot

MODEL AND APPARATUS

Two semispan wing-fuselage models were used during this investigation, namely, a 0.0714-scale model of the F8F-1 airplane and a 0.0893-scale model of the X-1 airplane. The geometric characteristics of the models used during these tests are shown in table I. The wings were made of solid aluminum and the fuselages were constructed of wood. Simplified models of the airplanes without canopies or tail surfaces were used. Photographs of the models investigated are shown in figure 1.

These models were mounted on a transonic bump in the Ames 16-foot high-speed wind tunnel. The bump is described in detail in reference 2. The aerodynamic forces and moments were measured by means of a strain-gage balance mounted inside the bump.

The fluctuating total pressures in the wake of the wings were measured with rakes. (See fig. 2.) Flush-type pressure cells similar to those used in the wake-measurement instrument are described in reference 3 and the electronic instrumentation is described in reference 4. The frequency response of this equipment has been extended to 300 cycles per second with ±5-percent accuracy. The fluctuating bending moments of the wings were measured by means of strain gages mounted on the wing surfaces near the root chord. (See fig. 3.)

TESTS

Range of Variables

The aerodynamic characteristics of the F8F-1 semispan wing-fuselage model were investigated for a Mach number range from 0.40 to 1.02 with a corresponding Reynolds number range of 1.4 to 2.2 million. The aerodynamic characteristics of the X-1 semispan wing-fuselage model were investigated for a Mach number range from 0.40 to 1.08 with a corresponding Reynolds number range of 1.1 to 1.9 million. The curves of Reynolds number variation with Mach number for these tests are shown in figure 4. The Reynolds number is based on the mean aerodynamic chord of the wing. Typical contours of local Mach number in the vicinity of the models on the bump are shown in figure 5. The angle-of-attack range for these tests varied from -2° to the highest positive angles allowed by the structural limitations of the model.

Reduction of Data

Calibration of all pressure cells showed linear response to external pressure or to vacuum, which was unchanged by the temperature variation in the range encountered during the tests. Only data from the center rake were analyzed because the outboard and inboard rakes did not operate satisfactorily. No pressure-cell response occurred as a result of the vibration of the wake instrument.

Lift forces, pitching moments, fluctuating bending moments, and fluctuating wake pressures are presented in coefficient form in figures 6 through 13. No tare corrections are applied to the force data. Blockage and tunnel-wall-interference effects are negligible since the models are extremely small in comparison with the tunnel test section. The indicated Mach number represents the Mach number at the 0.25 $\bar{c}$ of the wing. The angle of attack was corrected by -0.4° because of flow inclination over the bump.

The pitching-moment coefficients for the F8F-1 model are too large by an amount equal to 0.081 times the drag coefficient of the model. This correction could not be evaluated because of malfunctioning of the drag balance.

Wing fluctuating bending moments.- These moments were measured with calibrated strain gages and recorded by means of a multiple recording oscillograph. The three maximum peak-to-peak amplitudes of the traces were measured from each record and the averages of these amplitudes were converted to bending-moment-coefficient fluctuation (ΔC_B) and plotted as a function of Mach number at constant lift coefficients (fig. 12). The structural rigidity of the model wing affects the magnitude of the bending-moment fluctuations. It is thus necessary to find a criterion for which the effect of this structural-rigidity factor is negligible. For these models, the values of $\frac{\partial(\Delta C_B)}{\partial M}$ equals +0.05 and -0.05 were used. The lines connecting these points define the lower and upper limits, respectively, of the region of increased bending-moment fluctuations.

Fluctuating total-wake pressures.- The average fluctuating total pressures measured by the center rake in the wake of the wings have been recorded and analyzed in a manner similar to that described for the bending moments. These average amplitudes were converted to pressure-fluctuation coefficient $\left(\frac{\Delta h}{q}\right)$ and plotted as a function of Mach number at constant lift coefficients in figure 13. An arbitrary value of $\frac{\Delta h}{q} = 0.05$ was used to define both the lower and upper limits of the region of increased total-wake-pressure fluctuations.

[redacted]

RESULTS AND DISCUSSION

Static Aerodynamic Data

The static lift-force and pitching-moment characteristics of the models are presented in figures 6 through 11.

Buffet Boundaries

Shown in figure 12 is the variation of bending-moment-coefficient fluctuation versus Mach number at constant lift coefficients for the F8F-1 and the X-1 models. Plots showing the variation of pressure-fluctuation coefficient with Mach number at constant lift coefficients are shown in figure 13. Predicted boundaries, obtained as described in the last section, for both the F8F-1 and the X-1 models were obtained from figures 12 and 13, respectively. These estimated buffet boundaries are compared with buffet boundaries determined from flight-test data of full-scale airplanes in figure 14. For the F8F-1 model (fig. 14(a)) both methods of obtaining the buffet boundaries from wind-tunnel tests agree very well at low lift coefficients. However, disagreement is apparent with increase in lift coefficient. For the F8F-1 model at a lift coefficient of 0.5 the buffet boundaries are at Mach numbers of approximately 0.61, 0.63, and 0.66 as indicated by the fluctuating pressures in the wake, fluctuating bending moments, and flight data, respectively. For the F8F-1 model the bending-moment data appears to correlate better with the flight-determined buffet boundary throughout the test lift-coefficient range.

For the X-1 model in figure 14(b), the buffet boundary obtained from the fluctuating pressures in the wake gives the best correlation with the flight buffet boundary. At lift coefficient of 0.5, the lower buffet boundaries are at 0.78, 0.79, and 0.79 Mach numbers obtained from the fluctuating bending-moment data, fluctuating wake-pressure data, and flight data, respectively. The upper buffet boundaries at 0.97, 0.98, and 0.995 Mach numbers are obtained from the fluctuating wake-pressure data, flight data, and fluctuating bending-moment data, respectively.

It appears that buffet boundaries of full-scale airplanes can be estimated from fluctuating wing-bending moments and fluctuating wake pressures measured for relatively simple models in a wind tunnel. However, more wind-tunnel tests should be undertaken with models of other airplanes to obtain similar fluctuating data from which buffet boundaries may be determined, thereby substantiating or modifying the above methods. The fluctuating total pressures in the wake of the wings, from which buffet boundaries were determined, were measured by the center rake.

Two other rakes were provided but they did not operate satisfactorily during these tests so no measure of the effects of the spanwise location of the rake on the buffet boundaries was obtained. However, it was possible from existing data to see that buffeting was first indicated by the inboard rake pressure measurements and moved outboard toward the wing tips. In future tests of such models, the effects of spanwise location of the rake on the buffet boundaries predicted from wake-pressure fluctuation should be determined. Also, the effects of structural rigidity of the models upon the prediction of buffet boundaries should be considered.

CONCLUDING REMARKS

The results of this investigation indicate the following:

The buffet boundaries of the F8F-1 and the X-1 full-scale airplanes were estimated from fluctuating bending-moment data and fluctuating wake pressure data obtained for relatively simple models in a wind tunnel. These buffet boundaries are in reasonable agreement with those determined from flight tests of the full-scale airplanes. The fluctuating bending-moment data correlated better with flight determined results for the F8F-1 airplane whereas the fluctuating total pressures in the wake agreed with flight results more accurately for the X-1 airplane.

Ames Aeronautical Laboratory
National Advisory Committee for Aeronautics
Moffett Field, Calif.

REFERENCES

1. Gadeberg, Burnett L., and Ziff, Howard L.: Flight-Determined Buffet Boundaries of Ten Airplanes and Comparisons with Five Buffeting Criteria. NACA RM A50I27, 1951.

2. Axelson, John A., and Taylor, Robert A.: Preliminary Investigation of the Transonic Characteristics of an NACA Submerged Inlet. NACA RM A50C13, 1950.

3. Erickson, Albert L., and Robinson, Robert C.: Some Preliminary Results in the Determination of Aerodynamic Derivatives of Control Surfaces in the Transonic Speed Range by Means of a Flush-Type Electrical Pressure Cell. NACA RM A8H03, 1948.

4. Sorenson, Robert M., Wyss, John A., and Kyle, James C.: Preliminary Investigation of the Pressure Fluctuations in the Wakes of Two-Dimensional Wings at Low Angles of Attack. NACA RM A51G10, 1951.

TABLE I.- GEOMETRIC CHARACTERISTICS OF THE MODELS

	Models	
	F8F-1 (0.0714 scale)	X-1 (0.0893 scale)
Wing		
$\frac{S}{2}$, square feet	0.622	0.517
$\frac{b}{2}$, inches.	15.216	15.000
$\bar{c}$, inches	6.254	5.155
Aspect ratio	5.17	6
Root section	NACA 23019.26	NACA 65-108 (a=1)
Tip section.	NACA 23009	NACA 65-108 (a=1)
Root chord, inches	8.279	6.625
Tip chord, inches.	3.679	3.313
Incidence		
Root chord to thrust line, degrees	3	2.5
Tip chord to thrust line, degrees	3	1.5
Dihedral, degrees.	5.5	0
Washout, degrees	0	1
Unswept reference line	35-percent chord	40-percent chord
Taper ratio.	0.44	0.5
Fuselage		
Fineness ratio	4.9	6.7

NACA

[redacted]

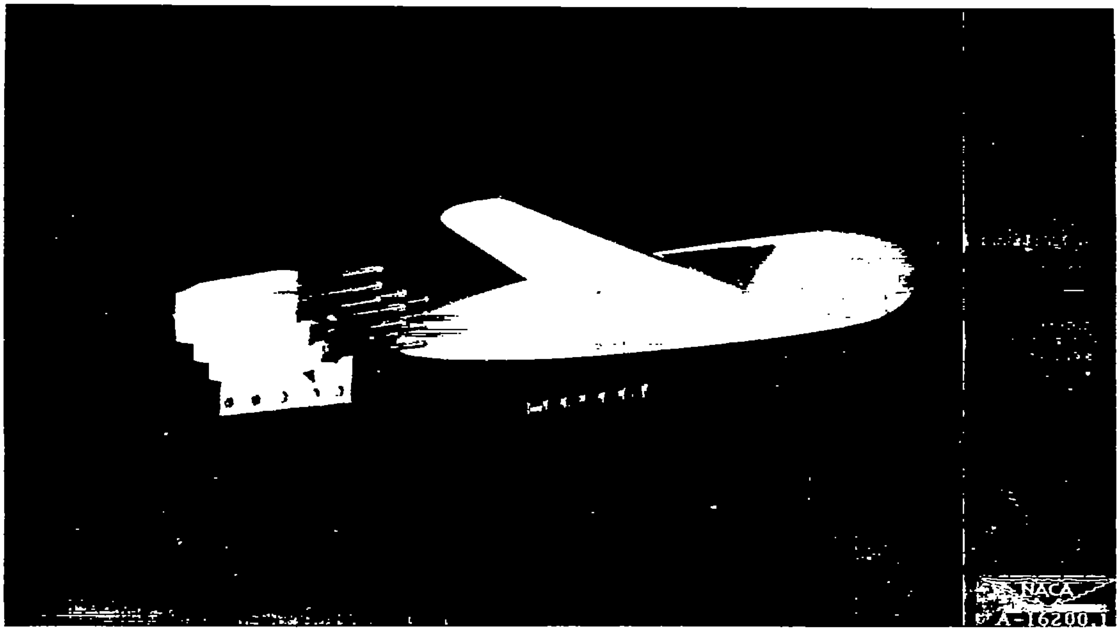

(a) The F8F-1 model.

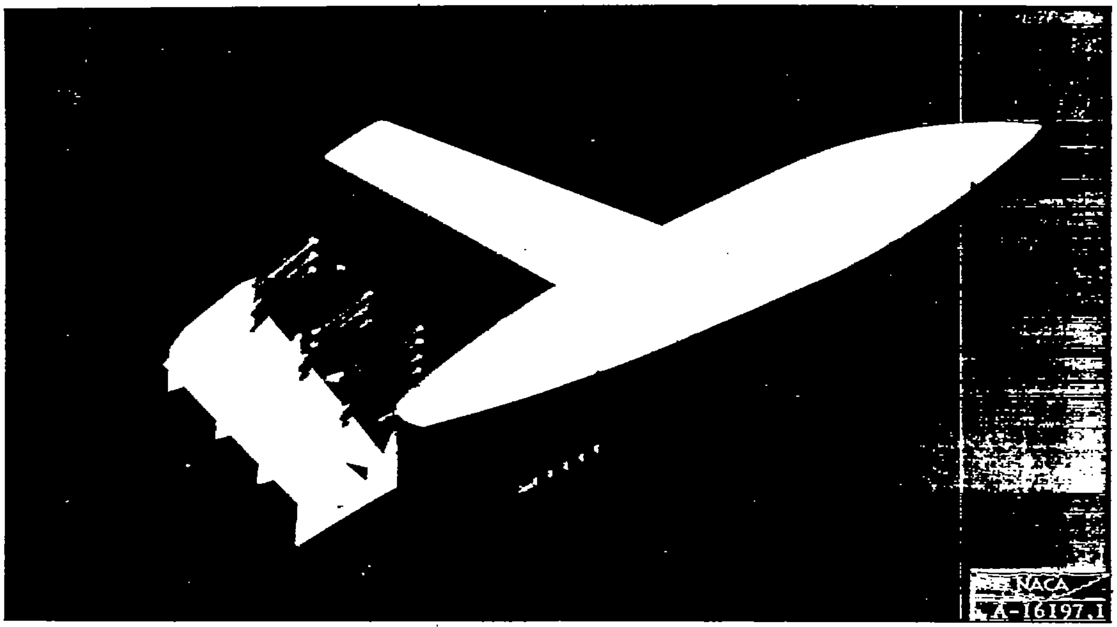

(b) The X-1 model.

Figure 1.– Photographs of the F8F-1 and X-1 models with the wake-measurement instrument.

[redacted]

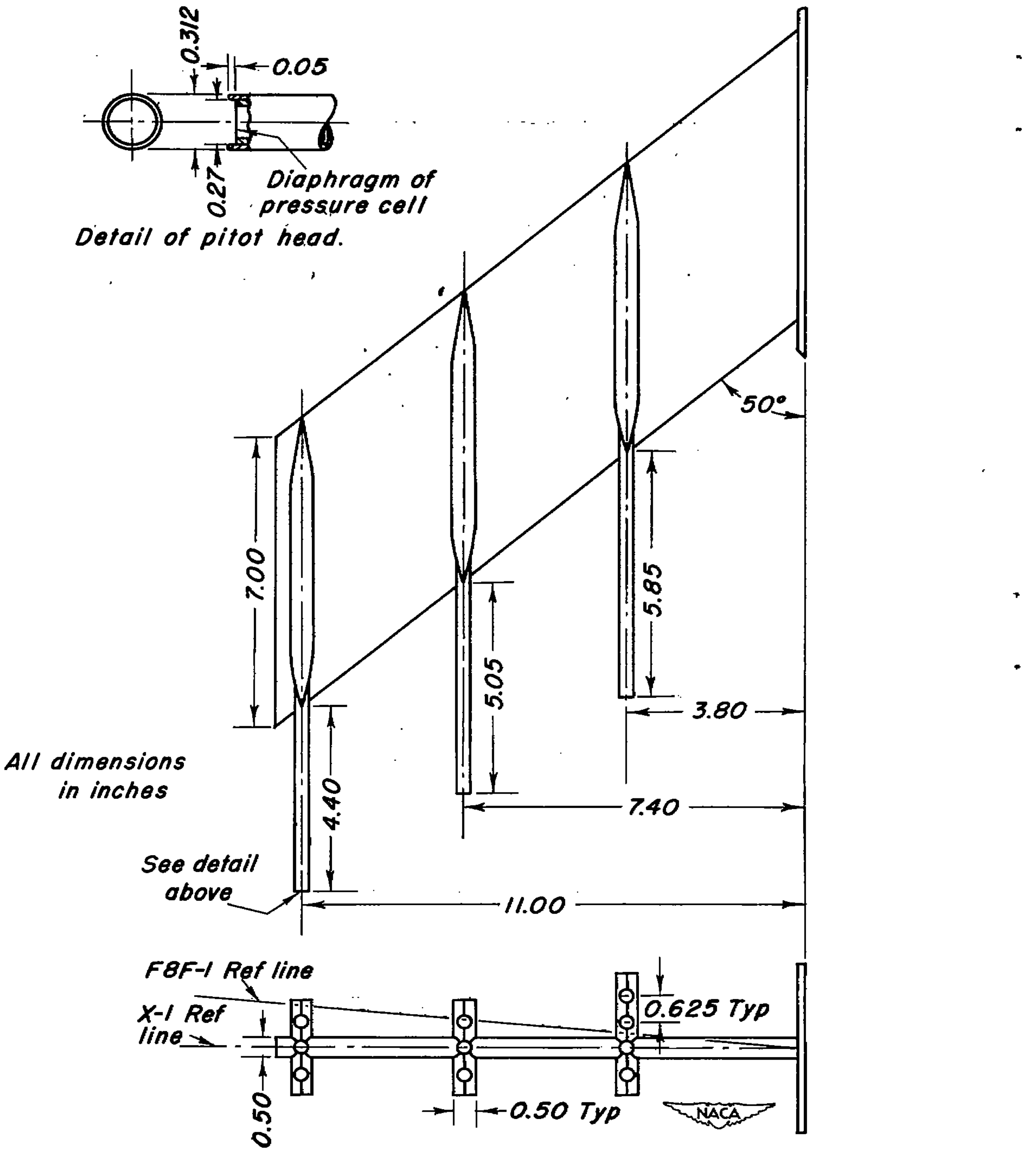

Figure 2.–Details of wake-measurement instrument.

[redacted]

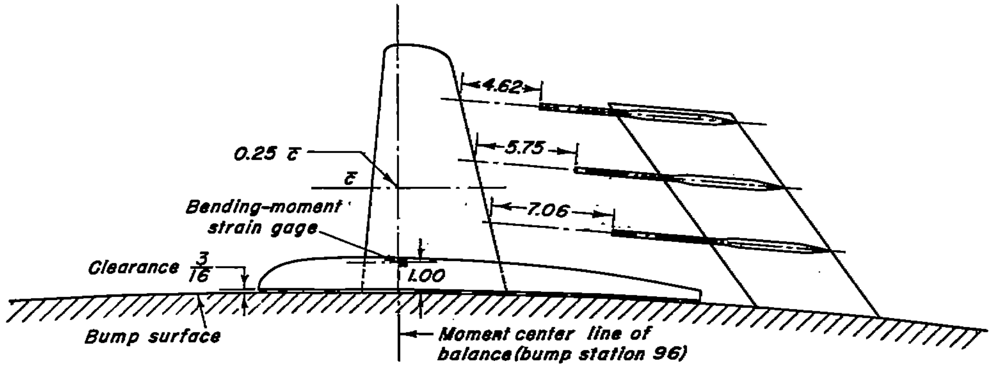

(a) F8F-1 model.

All dimensions in inches.

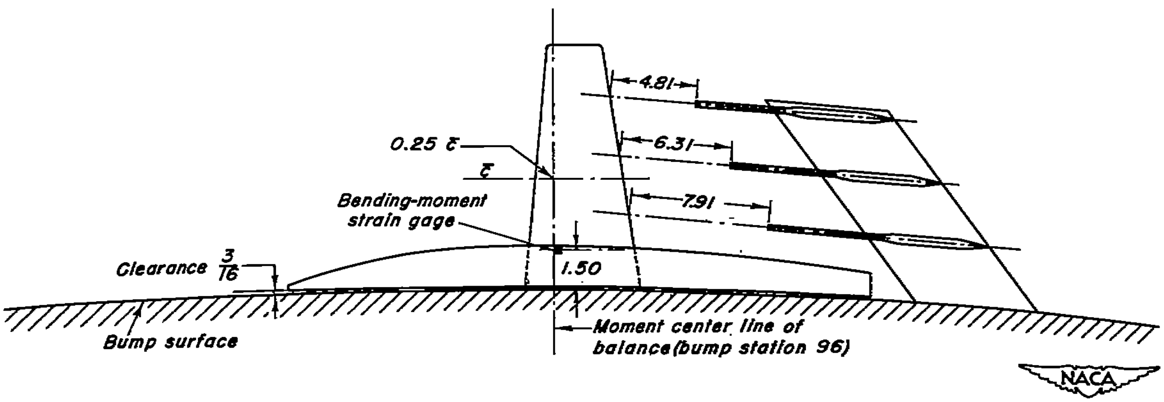

(b) X-1 model.

Figure 3.–Plan views of F8F-1 and X-1 models mounted on the transonic bump showing location of wake measurement instrument.

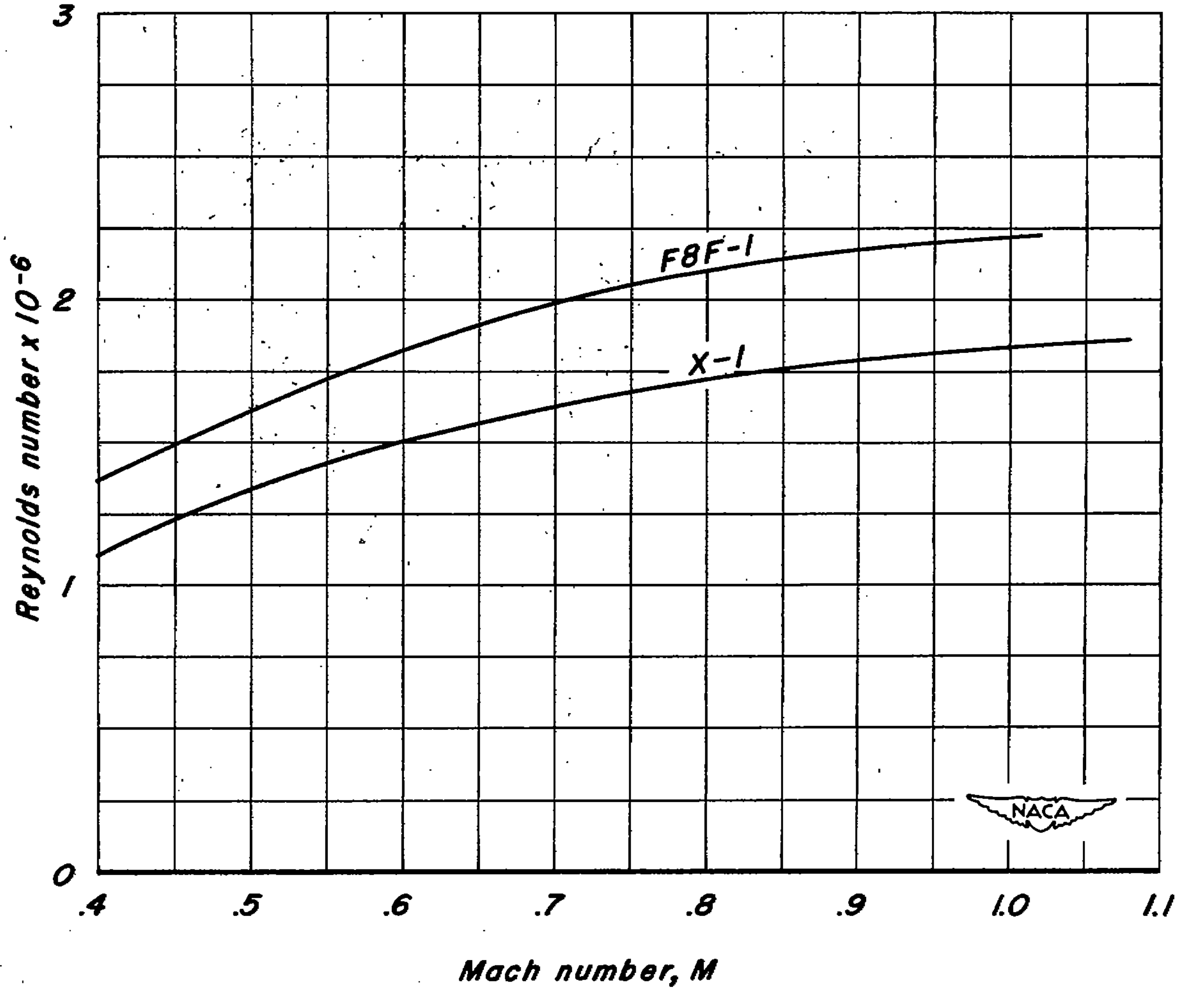

Figure 4.–The variation of Reynolds number with Mach number for the F8F-1 and X-1 models.

[redacted]

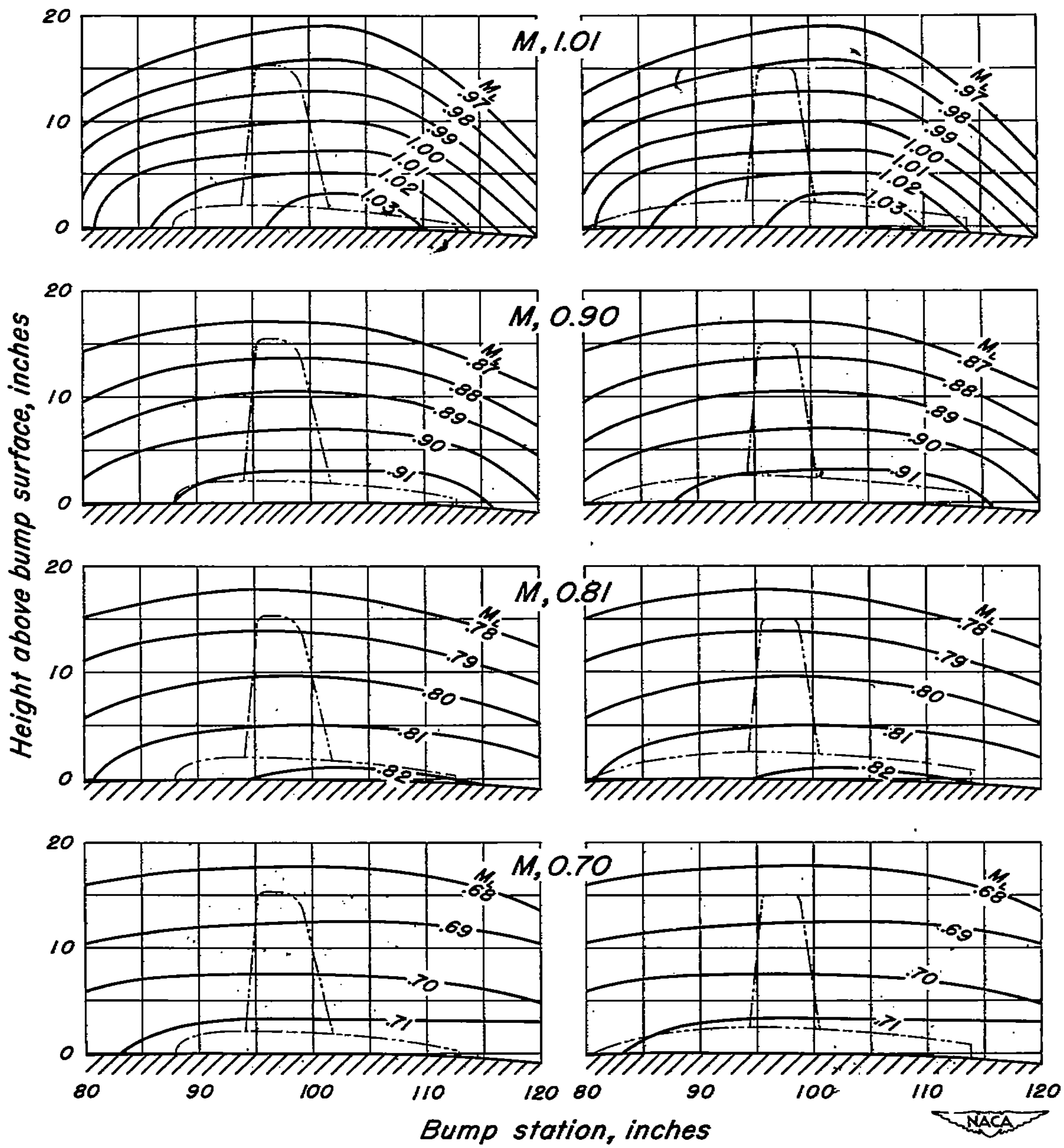

(a) F8F-1 model. (b) X-1 model.

Figure 5.–Typical Mach number contours over the transonic bump in the vicinity of the F8F-1 and X-1 models.

[redacted]

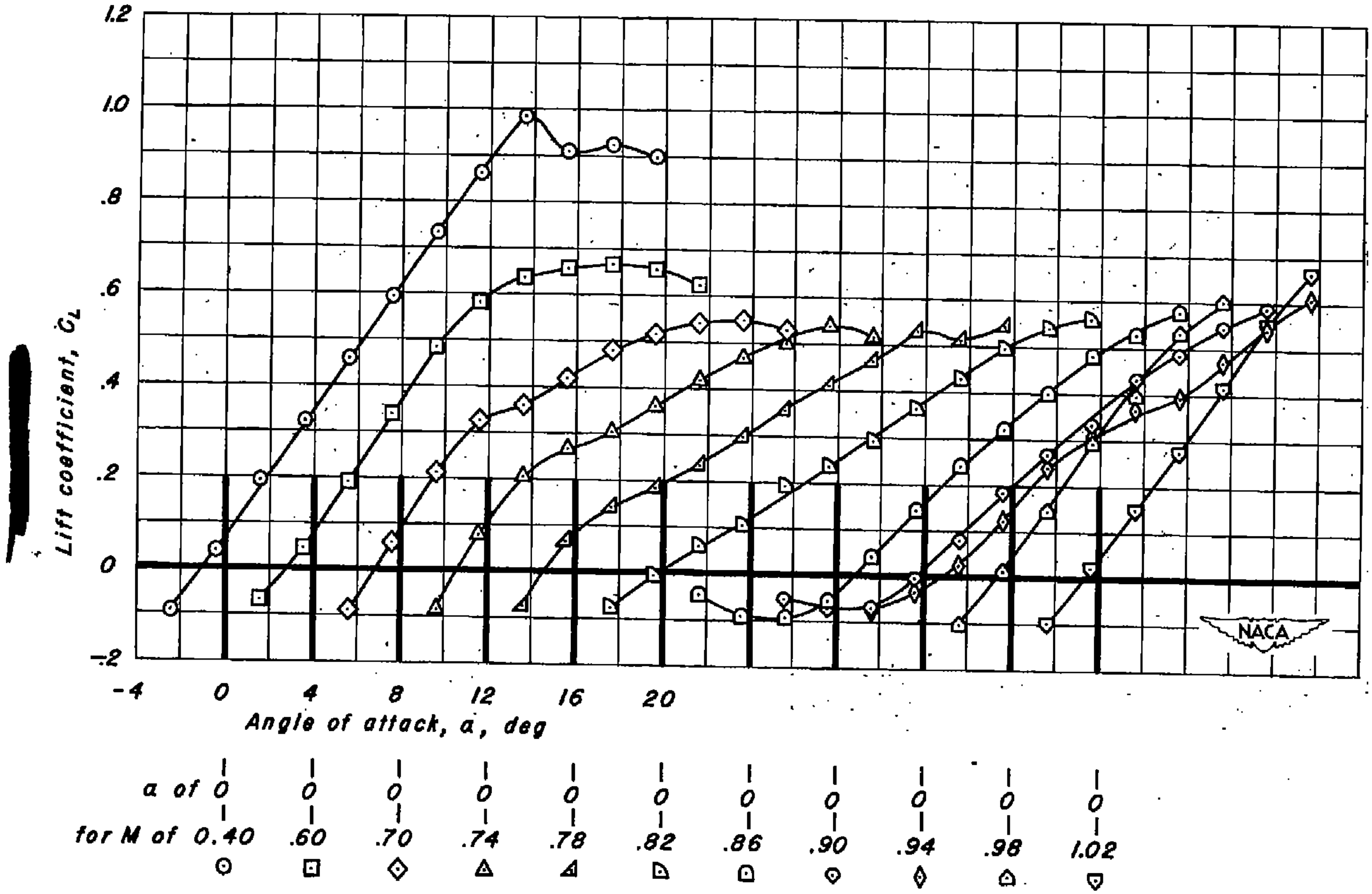

Figure 6.—Variation of lift coefficient with angle of attack at constant Mach numbers for the F8F-1 model.

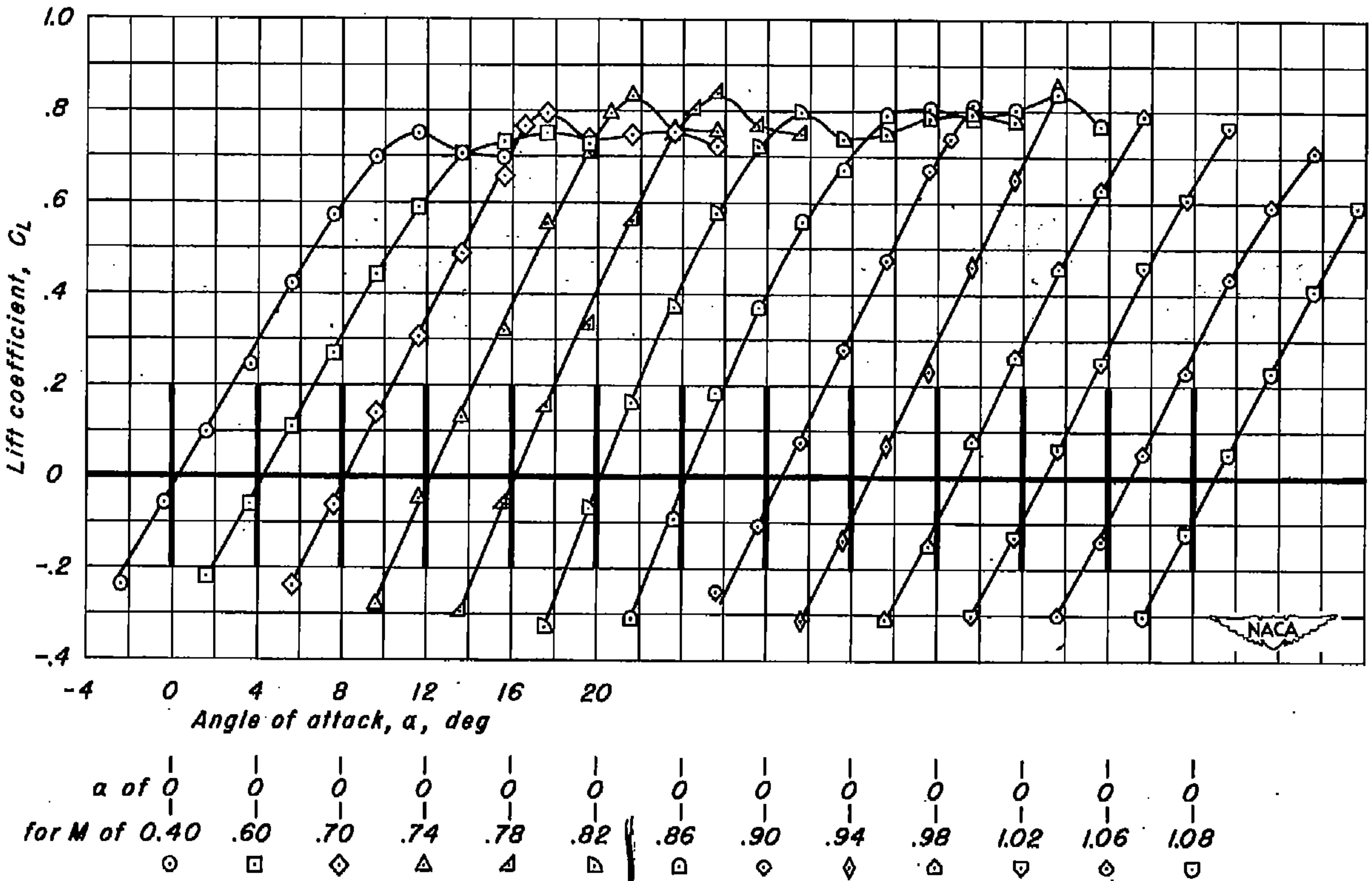

Figure 7.- Variation of lift coefficient with angle of attack at constant Mach numbers for the X-1 model.

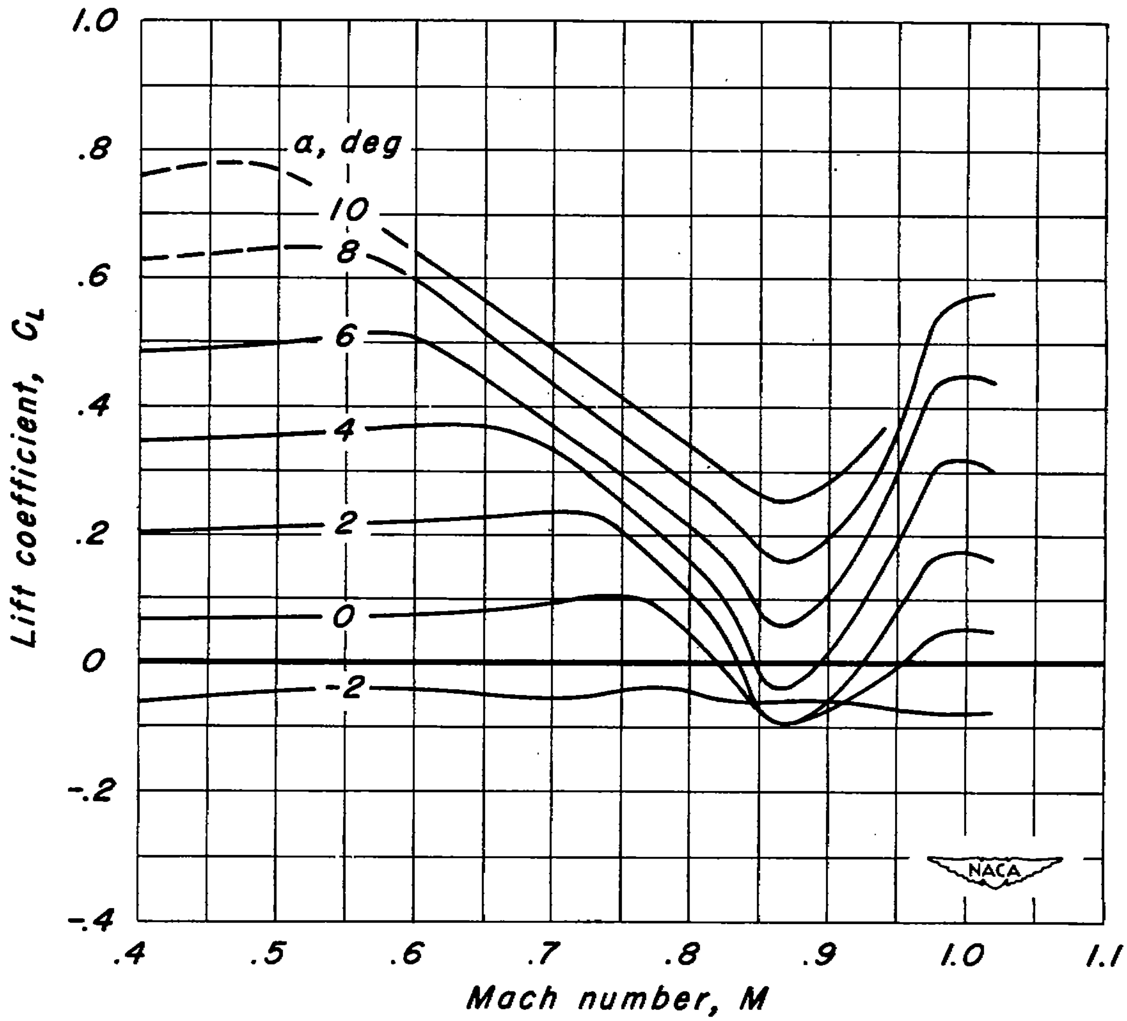

Figure 8.- Variation of lift coefficient with Mach number at constant angles of attack for the F8F-1 model.

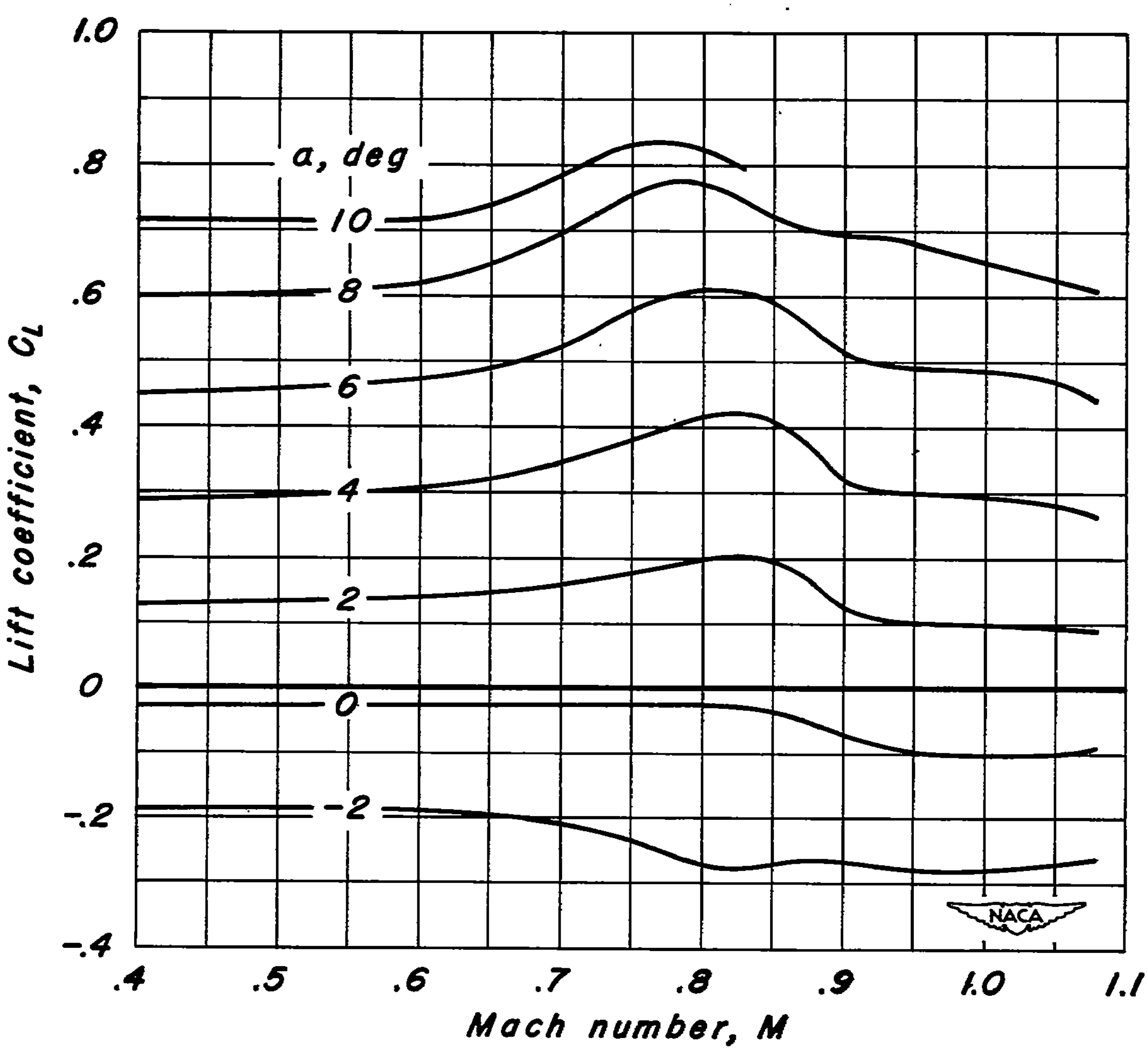

Figure 9.- Variation of lift coefficient with Mach number at constant angles of attack for the X-1 model.

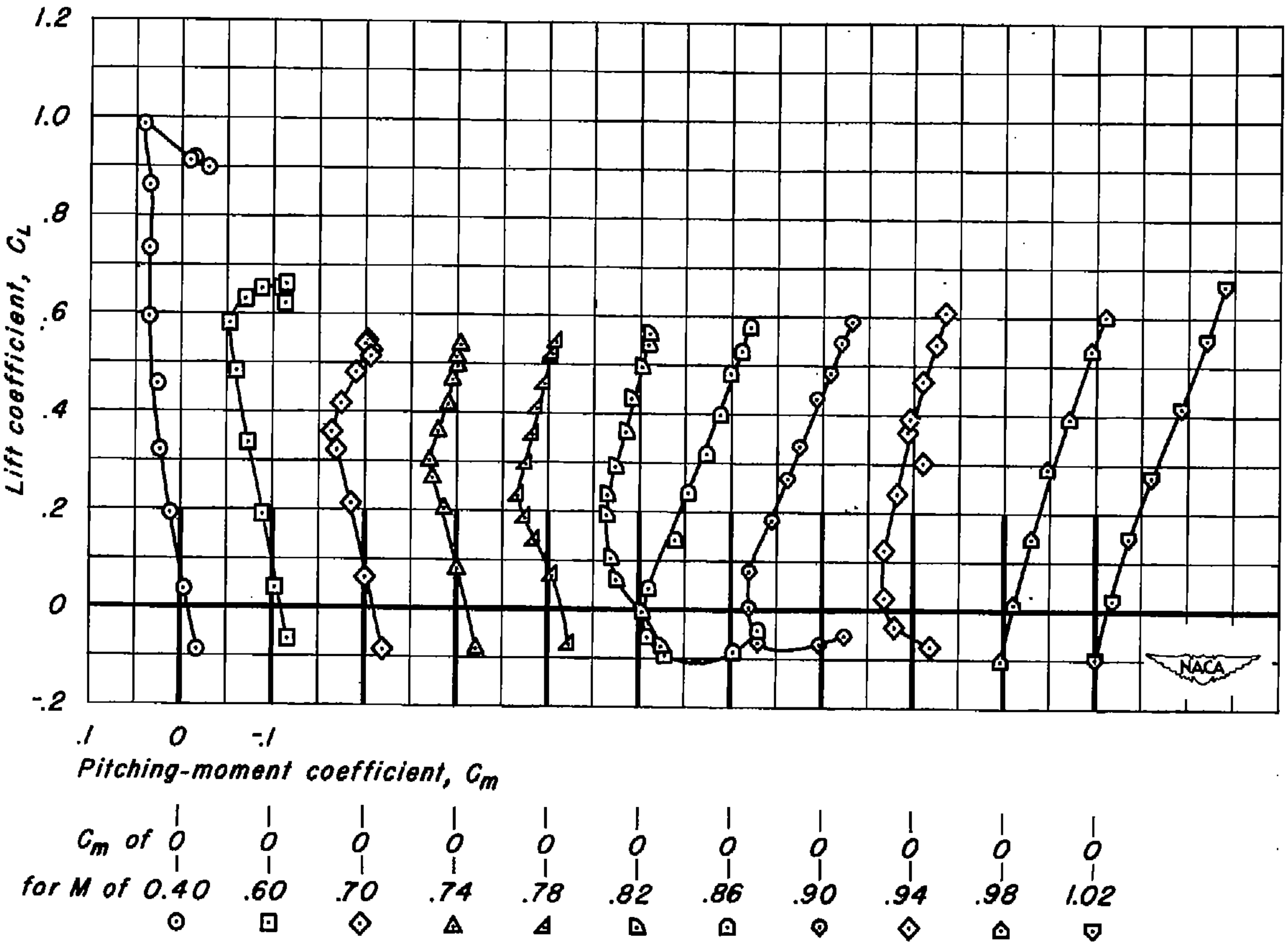

Figure 10.–Variation of lift coefficient with pitching-moment coefficient at constant Mach numbers for the F8F-1 model.

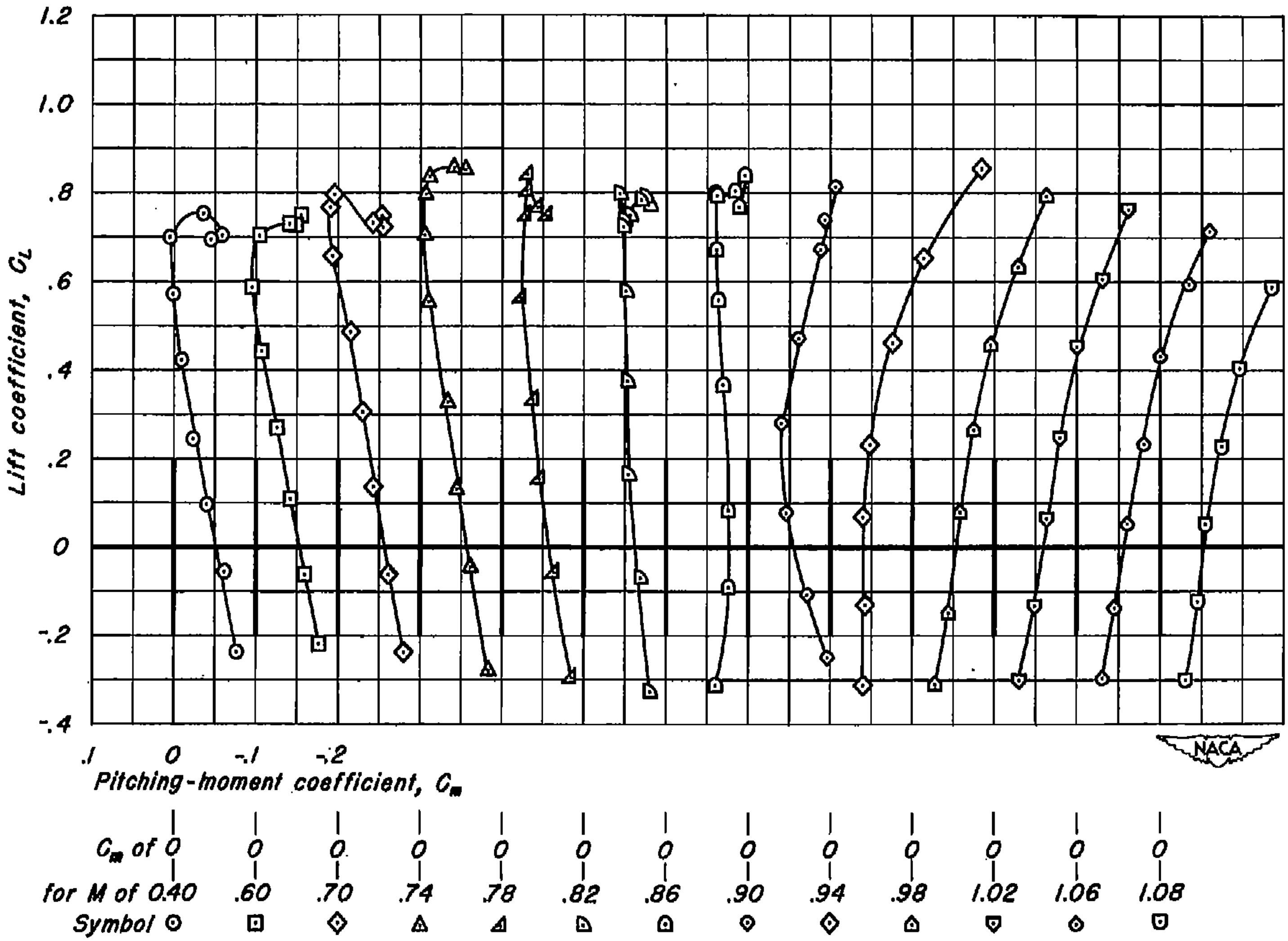

Figure 11.—Variation of lift coefficient with pitching-moment coefficient at constant Mach numbers for the X-1 model.

[redacted]

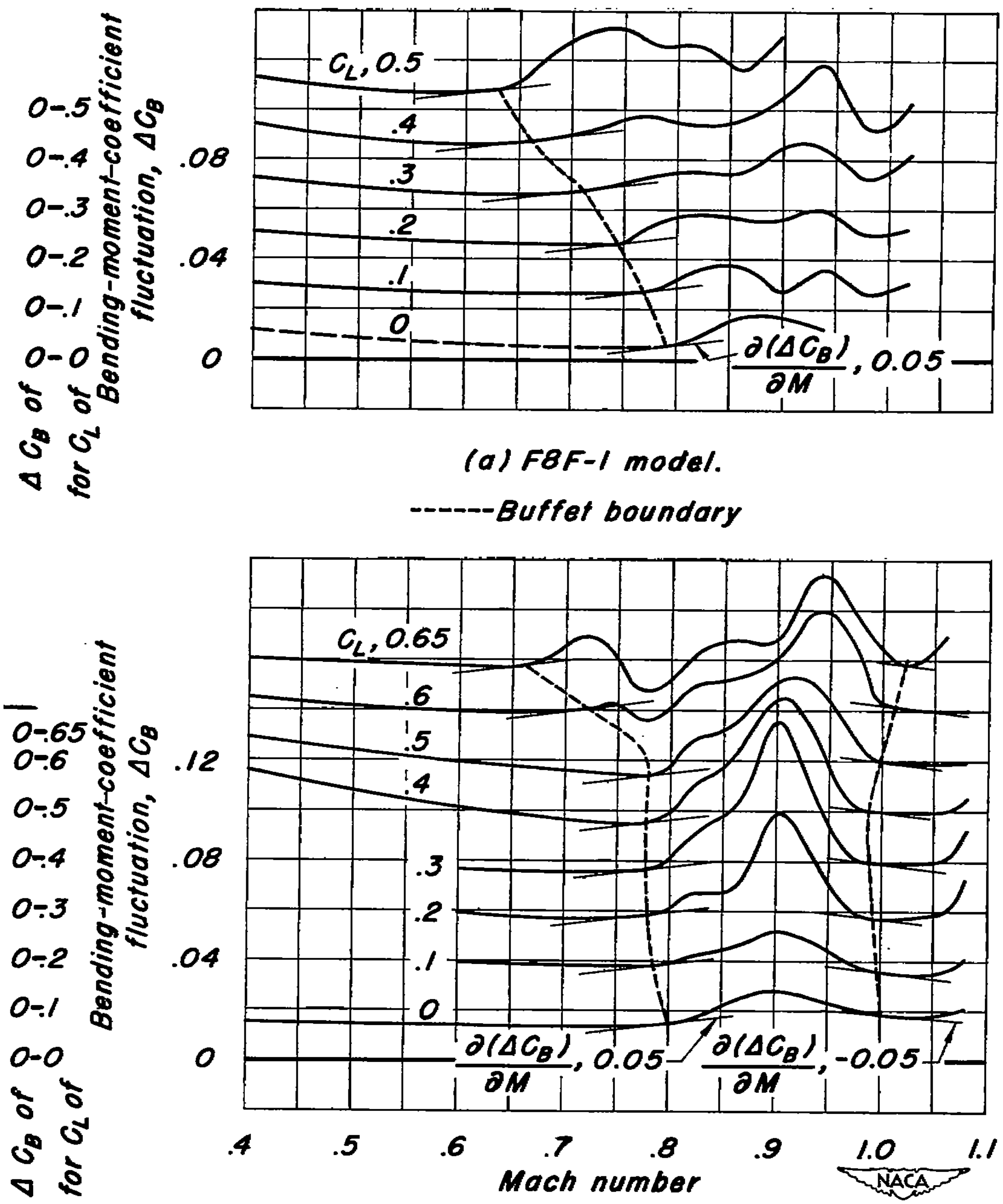

Figure 12.–The variation of bending-moment-coefficient fluctuation with Mach number at constant lift coefficients for the F8F-1 and the X-1 models.

[redacted]

[redacted]

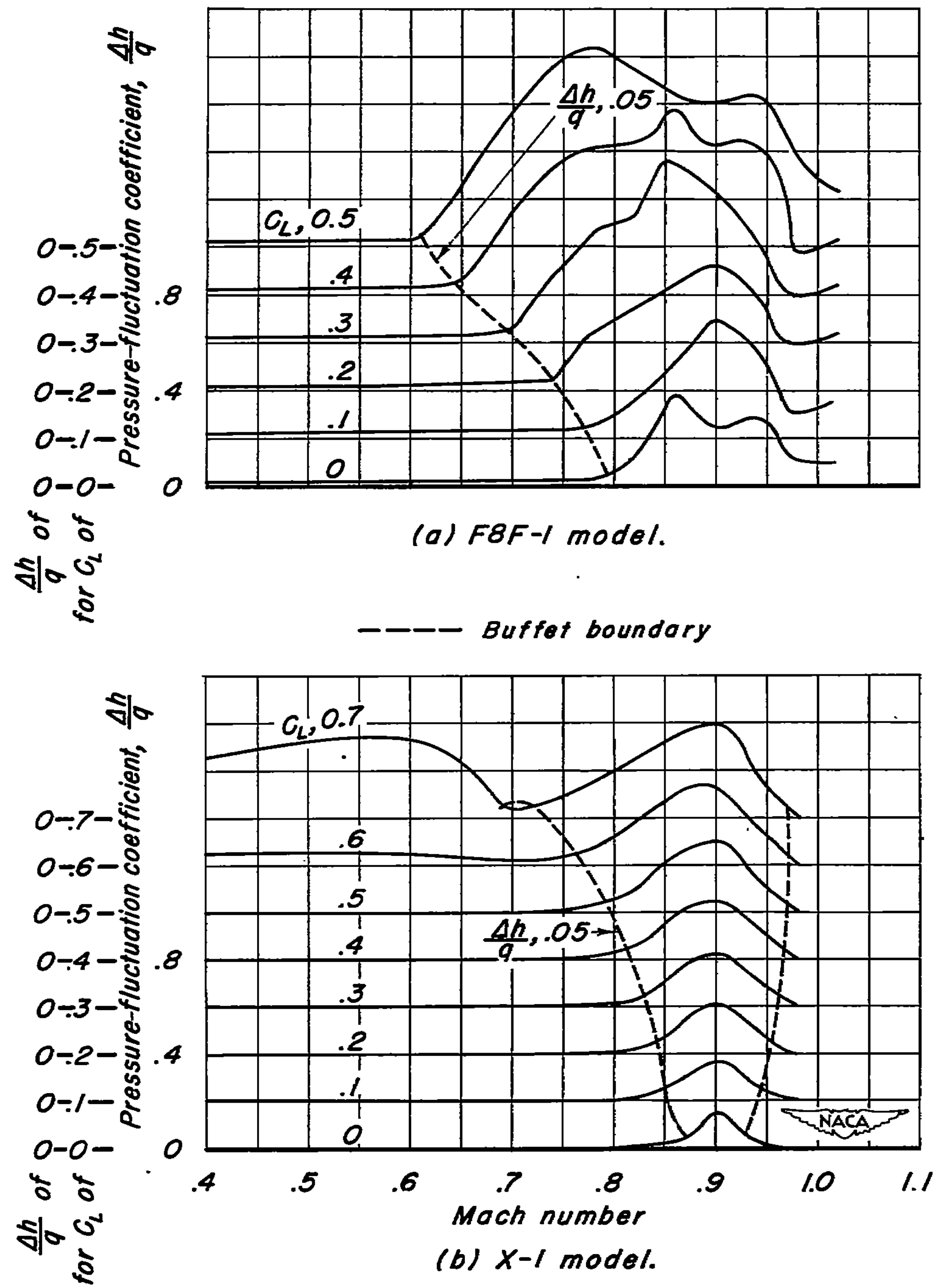

Figure 13.—The variation of pressure-fluctuation coefficient with Mach number at constant lift coefficients for the F8F-1 and the X-1 models.

[redacted]

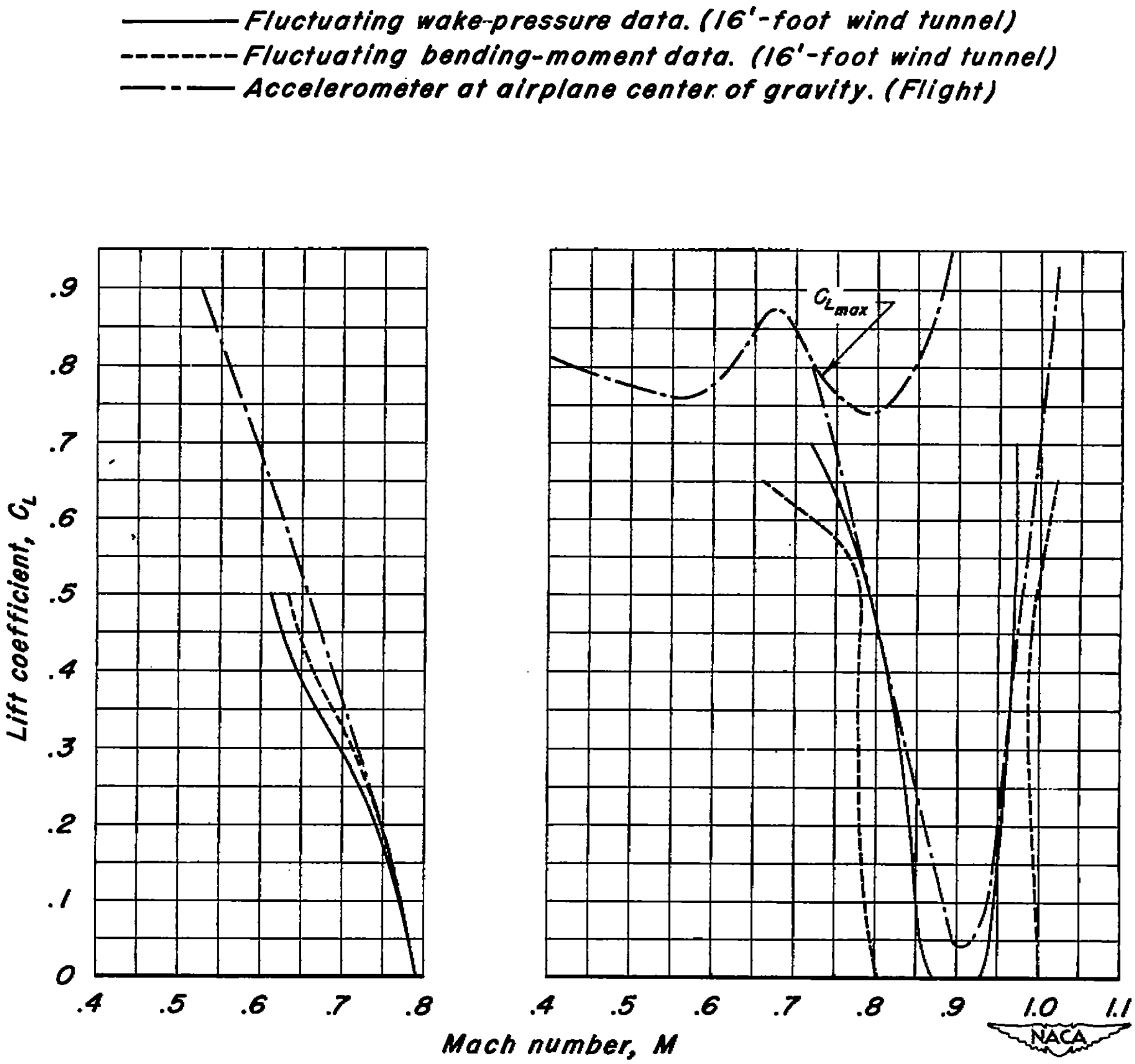

(a) F8F-1 airplane.

(b) X-1 airplane.

Figure 14.—Comparison of wind-tunnel buffet boundaries with flight buffet boundaries for the F8F-1 and X-1 airplanes.

[redacted]

SECURITY INFORMATION

[redacted]